High-speed low-voltage electro-optic modulator with a polymer-infiltrated silicon photonic crystal waveguide

Jan-Michael Brosi, Christian Koos, Lucio Claudio Andreani*, Michael Waldow†, Juerg Leuthold, and Wolfgang Freude

Institute of High-Frequency and Quantum Electronics, University of Karlsruhe, Germany,
**Department of Physics "A. Volta", University of Pavia, Italy*
†Now with RWTH Aachen, Germany.

j.brosi@ihq.uka.de, w.freude@ihq.uka.de

Abstract: A novel electro-optic silicon-based modulator with a bandwidth of 78 GHz, a drive voltage amplitude of 1 V and a length of only 80 μm is proposed. Such record data allow 100 Gbit/s transmission and can be achieved by exploiting a combination of several physical effects. First, we rely on the fast and strong nonlinearities of polymers infiltrated into silicon, rather than on the slower free-carrier effect in silicon. Second, we use a Mach-Zehnder interferometer with slotted slow-light waveguides for minimizing the modulator length, but nonetheless providing a long interaction time for modulation field and optical mode. Third, with this short modulator length we avoid bandwidth limitations by *RC* time constants. The slow-light waveguides are based on a photonic crystal. A polymer-filled narrow slot in the waveguide center forms the interaction region, where both the optical mode and the microwave modulation field are strongly confined to. The waveguides are designed to have a low optical group velocity and negligible dispersion over a 1 THz bandwidth. With an adiabatic taper we significantly enhance the coupling to the slow light mode. The feasibility of broadband slow-light transmission and efficient taper coupling has been previously demonstrated by us with calculations and microwave model experiments, where fabrication-induced disorder of the photonic crystal was taken into account.

OCIS codes: (130.0250) Optoelectronics; (130.3120) Integrated optics devices; (130.4110) Modulators; (130.5296) Photonic crystal waveguides; (130.5460) Polymer waveguides.

References and links

1. L. Liao, A. Liu, D. Rubin, J. Basak, Y. Chetrit, H. Nguyen, R. Cohen, N. Izhaky, and M. Paniccia, "40 Gbit/s silicon optical modulator for high-speed applications," Electron. Lett. **43**, 20072253 (2007).
2. B. Bortnik, Y.-C. Hung, H. Tazawa, B.-J. Seo, J. Luo, A. K.-Y. Jen, W. H. Steier, and H. R. Fetterman, "Electrooptic polymer ring resonator modulation up to 165 GHz," IEEE J. Sel. Top. Quantum Electron. **13,** 104–110 (2007).
3. D. Rezzonico, M. Jazbinsek, A. Guarino, O.-P. Kwon, P. Günter, "Electro-optic Charon polymeric microring modulators," Opt. Express **16,** 613–627 (2008), http://www.opticsexpress.org/abstract.cfm?URI=OPEX-16-2-613.
4. Y. Enami, C. T. Derose, D. Mathine, C. Loychik, C. Greenlee, R. A. Norwood, T. D. Kim, J. Luo, Y. Tian, A. K.-Y. Jen, and N. Peyghambarian, "Hybrid polymer/sol-gel waveguide modulators with exceptionally large electro-optic coefficients," Nature Photonics **1,** 180–185 (2007).

#92415 - $15.00 USD Received 4 Feb 2008; revised 10 Mar 2008; accepted 10 Mar 2008; published 12 Mar 2008

5. E. M. McKenna, A. S. Lin, A. R. Mickelson, R. Dinu, and D. Jin, "Comparison of r_{33} values for AJ404 films prepared with parallel plate and corona poling," J. Opt. Soc. Am. B **24,** 2888–2892 (2007).
6. T. Baehr-Jones, M. Hochberg, G. Wang, R. Lawson, Y. Liao, P. A. Sullivan, L. Dalton, A. K.-Y. Jen, and A. Scherer, "Optical modulation and detection in slotted silicon waveguides," Opt. Express **13,** 5216–5226 (2005), http://www.opticsexpress.org/abstract.cfm?URI=OPEX-13-14-5216.
7. G. Wang, T. Baehr-Jones, M. Hochberg, and A. Scherer, "Design and fabrication of segmented, slotted waveguides for electro-optic modulation," Appl. Phys. Lett. **91,** 143109 (2007).
8. Q. Xu, B. Schmidt, S. Pradhan, and M. Lipson, "Micrometre-scale silicon electro-optic modulator," Nature (London) **435,** 325–327 (2005).
9. B. Schmidt, Q. Xu, J. Shakya, S. Manipatruni, and M. Lipson, "Compact electro-optic modulator on silicon-on-insulator substrates using cavities with ultra-small modal volumes," Opt. Express **15,** 3140–3148 (2007), http://www.opticsexpress.org/abstract.cfm?URI=OPEX-15-6-3140.
10. K. K. McLauchlan and S. T. Dunham, "Analysis of a compact modulator incorporating a hybrid silicon/electro-optic polymer waveguide," IEEE J. Sel. Top. Quantum Electron. **12,** 1455–1460 (2006).
11. L. Gu, W. Jiang, X. Chen, L. Wang, and R. T. Chen, "High speed silicon photonic crystal waveguide modulator for low voltage operation," Appl. Phys. Lett. **90,** 071105 (2007).
12. M. Notomi, K. Yamada, A. Shinya, J. Takahashi, C. Takahashi, and I. Yokohama, "Extremely large group-velocity dispersion of line-defect waveguides in photonic crystal slabs," Phys. Rev. Lett. **87,** 253902 (2001).
13. J.-M. Brosi, J. Leuthold, and W. Freude, "Microwave-frequency experiments validate optical simulation tools and demonstrate novel dispersion-tailored photonic crystal waveguides," J. Lightwave Technol. **25,** 2502–2510 (2007).
14. V. R. Almeida, Q. Xu, C. A. Barrios, and M. Lipson, "Guiding and confining light in void nanostructure," Opt. Lett. **29,** 1209–1211 (2004).
15. L. C. Andreani and D. Gerace, "Photonic-crystal slabs with a triangular lattice of triangular holes investigated using a guided-mode expansion method," Phys. Rev. B **73,** 235114 (2006).
16. C. Koos, P. Vorreau, P. Dumon, R. Baets, B. Esembeson, I. Biaggio, T. Michinobu, F. Diederich, W. Freude, and J. Leuthold, "Highly-nonlinear silicon photonic slot waveguide," in Technical Digest of 2008 Optical Fiber Communication Conference and National Fiber Optic Engineers Conference, San Diego (CA), USA, Feb. 24–28, 2008, postdeadline paper PDP 25.
17. S. Hughes, L. Ramunno, J. F. Young, and J. E. Sipe, "Extrinsic optical scattering loss in photonic crystal waveguides: Role of fabrication disorder and photon group velocity," Phys. Rev. Lett. **94,** 033903 (2005).
18. L. H. Frandsen, A. V. Lavrinenko, J. Fage-Pedersen, and P. I. Borel, "Photonic crystal waveguides with semi-slow light and tailored dispersion properties," Opt. Express **14,** 9444–9450 (2006), http://www.opticsexpress.org/abstract.cfm?URI=OPEX-14-20-9444.
19. S. J. McNab, N. Moll, and Y. A. Vlasov, "Ultra-low loss photonic integrated circuit with membrane-type photonic crystal waveguides," Opt. Express **11,** 2927–2939 (2003), http://www.opticsexpress.org/abstract.cfm?URI=OPEX-11-22-2927.
20. G. Lecamp, J. P. Hugonin, and P. Lalanne, "Theoretical and computational concepts for periodic optical waveguides," Opt. Express **15,** 11042–11060 (2007), http://www.opticsexpress.org/abstract.cfm?URI=OPEX-15-18-11042.

1. Introduction

Fast Mach-Zehnder silicon modulators with low operating voltage fabricated in CMOS technology have the potential to considerably cut costs for high-speed optical transceivers. So far, the fastest broadband light modulation in silicon technology was achieved with free-carrier injection, which allowed modulation up to 30 GHz [1]. On the other hand, much higher modulation frequencies can be achieved with polymer based material systems through the virtually instantaneous electro-optic effect. And indeed, modulation at 165 GHz has been shown in a polymer ring resonator [2], however for a signal bandwidth of a few GHz only. Besides providing a fast electro-optic effect, polymers have a few more advantages. Poled polymers can have electro-optic coefficients ranging from moderate $r_{33} = 10\,\mathrm{pm/V}$ [3] to extremely high values of $r_{33} = 170\,\mathrm{pm/V}$ [4], [5], thus enabling operation with low drive voltage. Further, polymers can be infiltrated into silicon structures [6], [7]. This allows combining the highly nonlinear characteristics of polymers with the good high-index guiding properties of silicon-on-insulator devices. To reduce even further the structure size, the drive voltage, and the electrical power dissipation of polymer-silicon based modulators, resonant elements [8]-[10] or photonic crystals with low group velocity [11] may be employed.

#92415 - $15.00 USD Received 4 Feb 2008; revised 10 Mar 2008; accepted 10 Mar 2008; published 12 Mar 2008

In this paper we propose an ultra-compact silicon-based Mach-Zehnder amplitude modulator with a 78 GHz modulation bandwidth and a drive voltage of 1 V, which allows data transmission at 100 Gbit/s. This is achieved by infiltrating an electro-optic polymer into a slotted photonic crystal waveguide, thereby making use of the fast electro-optic effects of polymers, the strong field confinement in slotted waveguides and the slow light interaction enhancements provided by the photonic crystal waveguide, where group velocity and dispersion may be controlled [12], [13].

The paper is organized as follows: In Section 2, we introduce the Mach-Zehnder modulator. Section 3 explains the optimization strategy. Section 4 gives details of the slow-wave phase modulator design. In Section 5, modulator parameters like modulation bandwidth and π-voltage are discussed. Section 6 is devoted to performance data of an optimized integratable Mach-Zehnder modulator, and in Section 7 a taper is proposed for coupling efficiently to the slow-light mode of the phase modulator sections. The Appendix gives derivations of important relations.

2. The modulator

The configuration of the integrated Mach-Zehnder (MZ) interferometer (MZI) modulator (MZM) in silicon-on-insulator (SOI) technology is shown schematically in Fig. 1. The optical strip waveguides are operated in quasi-TE mode, where the optical field has a dominant electric field component E_x oriented parallel to the substrate plane. Y-branches split and combine the signals. Both arms of the MZ interferometer comprise phase modulator (PM) sections of length L. The PM sections consist of photonic crystal (PC) line defect (LD) waveguides (WG) with a narrow gap of width W_{gap} in the center, and are infiltrated with a $\chi^{(2)}$-nonlinear material (Pockels effect). In such a PC-WG, the dominant optical field component E_x is strongly confined to the gap (see Section 4). The nonlinear material is assumed to be poled [5] such that the axis of strongest electro-optic interaction (arrow $\Uparrow$ in Fig. 1) is aligned along the x-direction;

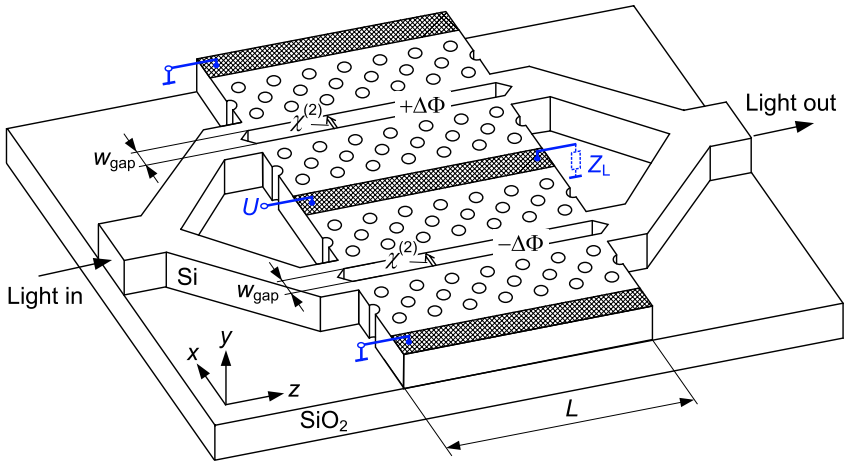

Fig. 1. Mach-Zehnder modulator schematic. The input WG carries a quasi-TE mode, the dominant electric field component of which (E_x) is oriented along the x-direction. A Y-branch (in reality an MMI coupler) splits the input into two arms where PC phase modulators are inserted. A coplanar transmission line provides electric bias and a modulation field driving the phase modulators in push-pull mode. The optical signals in both arms experience phase shifts $+\Delta\Phi$ and $-\Delta\Phi$.

#92415 - $15.00 USD Received 4 Feb 2008; revised 10 Mar 2008; accepted 10 Mar 2008; published 12 Mar 2008

the associated electro-optic coefficient is r_{33}. Therefore, only the x-components of the optical field and of the modulating field are relevant. The nonlinear material is assumed to respond instantaneously.

The silicon material of the PM sections is doped, e.g., with arsenic ($n_{\mathrm{D}} \approx 2 \times 10^{16}\,\mathrm{cm}^{-3}$), to be sufficiently conductive ($\sigma = 10\,\Omega^{-1}\,\mathrm{cm}^{-1}$) without introducing excessive optical loss. The edges of the PM silicon slabs are metalized with aluminum on top, and the three metallic layers (dark shading) running in parallel to the nonlinear optical WGs form a microwave coplanar waveguide (CPWG). The two outer electrodes are grounded, and a modulating voltage U applied to the center electrode generates a voltage wave that travels along the line and drives the PM sections in push-pull mode. In each of the arms, the electric modulation field $E_{\mathrm{el}} = U/W_{\mathrm{gap}}$ is dominantly oriented along the x-direction and almost completely confined to the gap. An optical quasi-TE field is launched at the input side of the MZM in Fig. 1. The phase shifts induced on the two MZI arms by the respective PMs are $+\Delta\Phi = +[\Delta\Phi_0 + \Delta\Phi(t)]$ and $-\Delta\Phi = -[\Delta\Phi_0 + \Delta\Phi(t)]$, where $\Delta\Phi(t) \sim U(t)$ represents the time-varying part. The bias voltage U_0 is chosen such that the offset point is set to $\Delta\Phi_0 = \pi/4$ (total phase difference $2\Delta\Phi_0 = \pi/2$ between both arms, MZ interferometer in quadrature). For switching the MZM from full transmission to full extinction, the phase in each PM section must be changed from $\Delta\Phi = -\pi/4$ to $\Delta\Phi = +\pi/4$, which corresponds to a voltage change from $U = -U_\pi/4$ to $U = +U_\pi/4$. The modulation voltage U that is required to change the phase in one modulator arm by π is called π-voltage U_π.

If the modulator is realized as shown in Fig. 1, the Y-junctions and the transitions from strip-WG to slow-light slot PC-WG lead to significant reflection and light scattering, and the mimimum feature sizes cannot be fabricated accurately. For a more practical design, the Y-branches should be replaced by MMI couplers. Further, an efficient transition from strip-WG to slow-light slot PC-WG is used as explained in Section 7.

3. MZM optimization strategy

An optimum MZM should provide large modulation bandwidth $f_{3\,\mathrm{dB}}$, require low modulation voltage amplitude U, should be fabricated based on CMOS processes, and it should have small size for easy on-chip integration. The MZM modulation bandwidth is in general limited by *RC*-effects and by the spatial walk-off between the electrical and optical waves. The spatial walk-off can be avoided by a travelling-wave design, where the group velocities $v_{\mathrm{g,\,el}}$ and $v_{\mathrm{g,\,opt}}$ of the electrical and optical waves are same, and where the CPWG is terminated with a matching impedance Z_{L} to avoid reflections.

However, such a travelling-wave structure with a well-terminated CPWG is difficult to realize, especially in a wide optical and electrical frequency range. If the modulator can be made sufficiently short in length L, a match of $v_{\mathrm{g,\,el}}$ and $v_{\mathrm{g,\,opt}}$ is not needed. We achieve this length reduction by using a PC line defect WG that is designed to have low optical group velocity and thus shows an increased electro-optic interaction. The maximum modulation frequency $f_{3\,\mathrm{dB}}$ is reached when the electrical modulation signal inside the electrical structure varies by more than half a period during the propagation time $t_{\mathrm{g,\,opt}} = v_{\mathrm{g,\,opt}}/L$ of the slow optical wave through the PM, see left-hand side of Eq. (1). This maximum frequency corresponds to the walk-off related bandwidth derived in Section 5 under the condition $v_{\mathrm{g,\,opt}} \ll v_{\mathrm{g,\,el}}$. In addition, we find that *RC*-effects do not play a significant role for our structure (see Appendix). Further, we derive in Section 5 and in the Appendix a relation for the π-voltage U_π, which in a simplified form is given by the right-hand side of Eq. (1),

$$f_{3\,\mathrm{dB}} \approx \frac{0.5}{t_{\mathrm{g,\,opt}}} = \frac{0.5\,v_{\mathrm{g,\,opt}}}{L}\,, \qquad U_\pi \propto \frac{W_{\mathrm{gap}}}{r_{33}}\,\frac{v_{\mathrm{g,\,opt}}}{L}\,. \tag{1}$$

#92415 - $15.00 USD Received 4 Feb 2008; revised 10 Mar 2008; accepted 10 Mar 2008; published 12 Mar 2008

From Eq. (1) we observe that the modulation bandwidth increases with the ratio $v_{\mathrm{g,\,opt}}/L$, however, at the expense of an increased π-voltage, i.e., a large drive voltage amplitude. For an optimum modulator (large bandwidth, low drive voltage) we need fixing the design bandwidth $f_{3\mathrm{dB}}$ first, i. e., we have to decide for a certain ratio $v_{\mathrm{g,\,opt}}/L$. The modulator length L is then directly related to the optical group velocity $v_{\mathrm{g,\,opt}}$, and a lower group velocity results in a shorter length. To reduce the π-voltage, a PM material with large nonlinear coefficient r_{33} needs to be chosen, and the gap width W_{gap} of the slotted waveguide should be made small. As we show in Section 4, both the optical and the microwave fields remain strongly confined to the nonlinear material, even for a narrow gap width W_{gap}. This is a specific advantage of the slotted PC-WG.

4. Slow-wave phase modulator

Figure 2 displays the slow-wave phase modulator section in more detail. In the center of a PC line defect WG, a narrow gap W_{gap} is cut out in form of a slot. The PC consists of a silicon slab with a triangular lattice of air holes having a lattice constant a. For a W_i line defect, a number of i rows of holes are omitted. The width W_1 of the resulting waveguide, see Fig. 2(b), depends on i, which need not be an integer. As explained previously, the silicon structure is covered with a highly nonlinear poled electro-optic polymer, which fills both the slot and the PC holes. Due to the high index-contrast between silicon ($n_{\mathrm{Si}} = 3.48$) and polymer ($n_{\mathrm{poly}} = 1.6$), the optical quasi-TE mode is mainly confined to the polymer-filled gap, Fig. 2(b) and [14].

For a minimum modulation voltage U we need to avoid any voltage drop in the silicon material between the electrodes (Al in Fig. 2(a)) and the gap. To this end, the silicon must be made sufficiently conductive by doping. Choosing then the smallest possible gap that is still compatible with technological constraints, and selecting a polymer with a large linear electro-optic coefficient minimizes the π-voltage U_π, Eq. (1).

While maintaining the low group velocity of the optical mode, the PC-WG can be adjusted such that chromatic dispersion of the optical wave is negligible, and signal distortions are avoided. In Section 6 it is shown that such a design leads to a large MZM bandwidth $f_{3\mathrm{dB}} = 78\,\mathrm{GHz}$ for a drive voltage amplitude as small as $\hat{U} = U_\pi/4 = 1\,\mathrm{V}$. For explaining our PC waveguide design decisions, the following two subsections describe first a slow-wave PC slot waveguide PM and its properties, and then discuss the optimized PC slot waveguide design for a flattened dispersion curve.

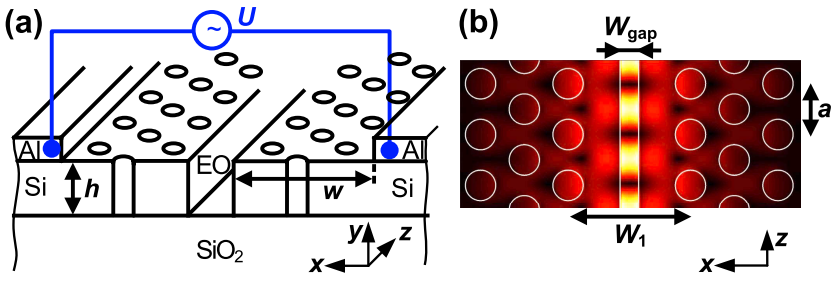

Fig. 2. Phase modulator (a) schematic and (b) dominant electric field component E_x. A slot filled with an electro-optic polymer (EO) of width W_{gap} is cut in a silicon photonic crystal line-defect waveguide of width W_1. The silicon slabs of height h and width w are doped for electrical conductivity and contacted with aluminum layers. E_x is strongly confined to the slot. The phase $\Delta\Phi$ of the propagating optical wave is tuned by applying a voltage to the polymer. The triangular-lattice period is a.

#92415 - $15.00 USD Received 4 Feb 2008; revised 10 Mar 2008; accepted 10 Mar 2008; published 12 Mar 2008

4.1. PC slot waveguide

PC waveguides lend themselves easily to a reduced group velocity near the edge of the Brillouin zone. A conventionally designed PC slot WG usually supports a mode with low group velocity, indeed. For a line-defect width W_1 chosen to correspond to a W1.4 LD WG, the associated band diagram is displayed in Fig. 3. The low group velocity region is marked by an oval to the right. The figure is calculated with the guided-mode expansion (GME) method [15], and simulations with the finite integration technique (FIT) verify the results.

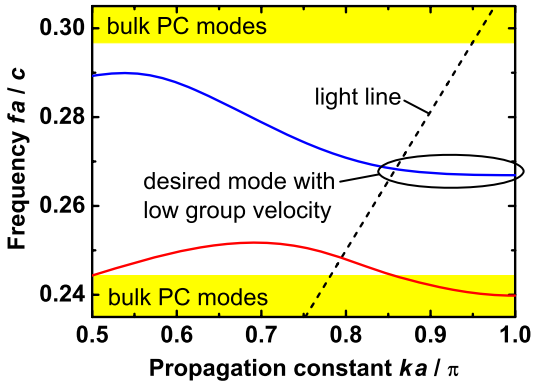

Fig. 3. Band diagram of W1.4 PC slot waveguide. The desired mode exhibits a low group velocity below the light line of the polymer cladding. PC slab height $h = 220\,\mathrm{nm}$, polymer gap width $W_{\mathrm{gap}} = 150\,\mathrm{nm}$, PC lattice period $a = 408\,\mathrm{nm}$, hole radii $r/a = 0.3$, line defect width $W_1 = 1.4\sqrt{3}a$. The polymer refractive index is $n_{\mathrm{poly}} = 1.6$, f, k, c denote frequency, propagation constant and vacuum speed of light, respectively.

The group velocity of the mode inside the marked region of Fig. 3 is displayed in Fig. 4(b) as a function of frequency (dashed line). The group velocity varies between nearly 0 % and 6 % of the vacuum speed of light c in the region below the light line. However, a high chromatic dispersion of $C > 5\,\mathrm{ps}/(\mathrm{mm\,nm})$ is also observed.

4.2. PC slot waveguide with dispersion flattening

For a better design with a lower chromatic dispersion, we optimize the hole radii $r_{1,2,3}$ and the distances between the hole centers $W_{1,2,3}$, see Fig. 4(a). As a result of the optimization process we find a set of W1.25 WGs that all provide a low group velocity over a wide spectral range. The frequency dependence of the resulting group velocity with various radii r_2 as parameters is shown in Fig. 4(b). An increase of the parameter r_2 decreases the group velocity, while a flat dispersion is maintained. For the value $r_2/a = 0.36$, the group velocity is 4 % of the vacuum speed of light c over a bandwidth of about 1 THz. It is also possible to obtain a negative chromatic dispersion, which is for example the case for $r_2/a = 0.30$ or $r_2/a = 0.38$, Fig. 4(b). For all presented designs, the air hole diameters are larger than 200 nm in order to meet fabrication constraints. The concept of the PC-WG with broadband low group velocity was experimentally verified previously [13].

#92415 - $15.00 USD Received 4 Feb 2008; revised 10 Mar 2008; accepted 10 Mar 2008; published 12 Mar 2008

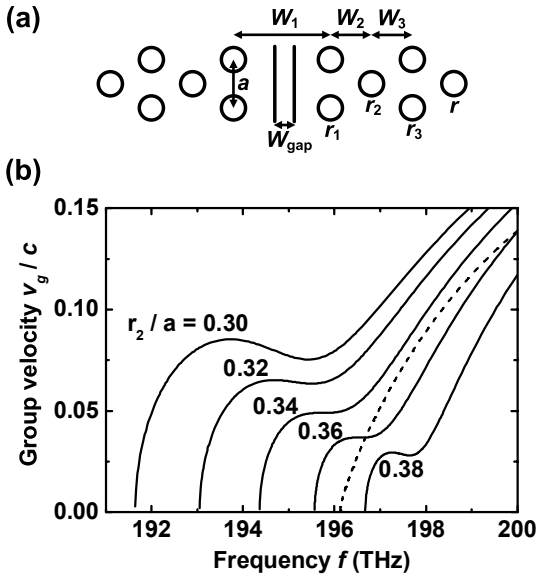

Fig. 4. W1.25 PC slot waveguide with slab height $h = 220\,\text{nm}$, polymer gap width $W_{\text{gap}} = 150\,\text{nm}$, PC lattice period $a = 408\,\text{nm}$. (a) Structure parameters and (b) group velocity as a function of frequency with varying hole radii r_2. With $r_2/a = 0.36$, the group velocity amounts to 4% of the vacuum speed of light c, and the group velocity dispersion is negligible in a bandwidth of 1 THz. For comparison, the group velocity of the conventional W1.4-WG of Fig. 2 is plotted as a dashed line ($W_1 = 1.4\sqrt{3}a$, $W_2 = W_3 = 0.5\sqrt{3}a$, $r_1 = r_2 = r_3 = r = 0.3a$). Parameters of the W1.25-WG are $W_1 = 1.25\sqrt{3}a$, $W_2 = 0.65\sqrt{3}a$, $W_3 = 0.45\sqrt{3}a$, $r_1 = 0.25a$, $r_3 = r = 0.3a$.

5. Modulator performance parameters

The main performance parameters for the modulator are the MZM modulation bandwidth $f_{3\,\text{dB}}$ and the phase modulator π-voltage U_π. The two parameters are derived and discussed in this section.

5.1. Modulation bandwidth of Mach-Zehnder modulator

The bandwidth of the MZM is limited by the walk-off between electrical and optical waves. *RC* limitations do not play a role for the presented structures as has been shown in the Appendix. The walk-off limited bandwidth depends on the termination of the CPWG, and here we discuss the two cases of a matched load and an open.

1) Walk-off bandwidth, CPWG with matched load

The CPWG be ideally terminated with a matched load so that the modulating wave traveling along z is not reflected at the end of the CPWG and maintains a spatially constant amplitude $|U|$. Electrical and optical waves propagate in the same direction, but in general at different group velocities $v_{\text{g, el}}$ and $v_{\text{g, opt}}$ (group delays $t_{\text{g, el}}$ and $t_{\text{g, opt}}$ over the PM section length L). The nonlinear interaction is maximum for co-directionally traveling waves (TW) with $t_{\text{g, el}} = t_{\text{g, opt}}$, and it decreases strongly if $t_{\text{g, el}} \neq t_{\text{g, opt}}$. When the electrical and optical signal envelopes have acquired a phase difference of π, the limiting modulating frequency $f_{3\,\text{dB}}$ is reached with

#92415 - $15.00 USD Received 4 Feb 2008; revised 10 Mar 2008; accepted 10 Mar 2008; published 12 Mar 2008

$\omega_{3\,\mathrm{dB}}^{(\mathrm{TW})}|t_{\mathrm{g,\,opt}}-t_{\mathrm{g,\,el}}|=\pi$, i. e.,

$$f_{3\,\mathrm{dB}}^{(\mathrm{TW})}=\frac{0.5}{|t_{\mathrm{g,\,opt}}-t_{\mathrm{g,\,el}}|}=\frac{0.5\,v_{\mathrm{g,\,opt}}}{L}\,\frac{1}{|1-v_{\mathrm{g,\,opt}}/v_{\mathrm{g,\,el}}|}\,. \tag{2}$$

Following the formalism in [16], a more accurate formula can be derived, whereby it is shown that the factor of 0.5 in Eq. (2) need be replaced by 0.556.

2) Walk-off bandwidth, CPWG with open-circuit

In order to keep the design of an integratable MZM simple, the CPWG would be more favourably be configured without terminating resistances. Because of the reflection at the open CPWG, a standing wave results. For the forward propagating part of the electrical wave, Eq. (2) specifies the limiting frequency. However, the backward propagating wave puts a tighter walk-off limit, because now the electrical wave has the opposite direction compared to the optical wave. With similar arguments that led to Eq. (2) we find $\omega_{3\,\mathrm{dB}}|t_{\mathrm{g,\,opt}}+t_{\mathrm{g,\,el}}|=\pi$,

$$f_{3\,\mathrm{dB}}=\frac{0.5}{|t_{\mathrm{g,\,opt}}+t_{\mathrm{g,\,el}}|}=\frac{0.5\,v_{\mathrm{g,\,opt}}}{L}\,\frac{1}{|1+v_{\mathrm{g,\,opt}}/v_{\mathrm{g,\,el}}|}\,. \tag{3}$$

As above, a more accurate formula can be developed following [16] where the factor of 0.5 in Eq. (3) is again replaced by 0.556. If $v_{\mathrm{g,\,opt}}\ll v_{\mathrm{g,\,el}}$ holds, then $f_{3\,\mathrm{dB}}\approx f_{3\,\mathrm{dB}}^{(\mathrm{TW})}$ and electrically short MZM designs with and without matching load for the CWPG become nearly equivalent, resulting in Eq. (1).

5.2. π-voltage U_π of phase modulator

A Mach-Zehnder modulator's sensitivity is characterized by the π-Voltage U_π of its phase modulators. For a given PM length L the voltage $|U|$ needed for a π-phase shift is defined to be U_π. For large modulation sensitivity, U_π should be small. An optical wave propagating through a PM experiences a nonlinear refractive index change Δn in proportion to the electric modulating field E_{el} inside the nonlinear PM material,

$$\Delta n=-\frac{1}{2}r_{33}\,n_{\mathrm{poly}}^3\,E_{\mathrm{el}},\qquad E_{\mathrm{el}}=U/W_{\mathrm{gap}}\,. \tag{4}$$

As before, n_{poly} represents the effective linear part of the refractive index in the PM section, and r_{33} is the (scalar) linear electro-optic coefficient. The total phase shift of the optical wave due to the index change in a PM section of length L is (following the formalism in Appendix Section A and in [16])

$$\Delta\Phi=-\Delta\beta L=-\Gamma\Delta n k_0 L\,. \tag{5}$$

The quantity $k_0=2\pi f_0/c$ is the vacuum wave number. In the process of deriving Eq. (5) the so-called field interaction factor Γ was introduced. It quantifies the strength of the nonlinear electro-optic interaction of modulating field and optical mode in a cross-section A along a lattice period a (see Appendix Eqs. (8)-(13) and [16]),

$$\Gamma=\int_{\mathrm{gap}}\frac{n}{Z_0}|\hat{E}_x|^2\,\mathrm{d}V\Bigg/\int a\,\Re(\hat{\mathbf{E}}\times\hat{\mathbf{H}}^*)\cdot\mathbf{e}_z\,\mathrm{d}A\propto\frac{1}{v_{\mathrm{g,\,opt}}}\,. \tag{6}$$

In Eq. (6), Z_0 is the free-space wave impedance, $\hat{\mathbf{E}}$ (x-component E_x) and $\hat{\mathbf{H}}$ are the optical modal electric and magnetic fields, and $\mathbf{e}_z$ is the unit vector in z-direction. The field *interaction* factor Γ as defined in Eq. (6) is different from the field *confinement* factor, which is usually calculated as a ratio between the optical power in the cross-section of the interaction region

#92415 - $15.00 USD Received 4 Feb 2008; revised 10 Mar 2008; accepted 10 Mar 2008; published 12 Mar 2008

and the total power propagating in the whole modal cross-section. While the field confinement factor varies between 0 and 1, the field interaction factor Γ can be larger than 1. The integral in the numerator of Eq. (6) is a measure of the energy stored in the transverse component of the propagating optical mode inside the PM along a length a (see Appendix, Eq. (16)). The denominator represents the transported power in the modal cross-section. According to Eq. (17), the energy stored in a volume, when related to the cross-section power of a wave that crosses this volume, increases in proportion to the reciprocal group velocity of the wave. Because in the numerator of Γ only the dominant transverse field component is regarded, the proportionality $\Gamma \propto 1/v_{\mathrm{g,\,opt}}$ holds only approximately. Application of a voltage U_π to the PM results by definition in a phase change of $\Delta\Phi = \pi$ within a length L. From Eq. (4)-(6), the π-voltage is computed to be

$$U_\pi = \frac{c}{n_{\mathrm{poly}}^3 f_0}\,\frac{W_{\mathrm{gap}}}{r_{33}}\,\frac{1}{L\Gamma}, \qquad U_\pi \propto \frac{W_{\mathrm{gap}}}{r_{33}}\,\frac{1}{L\Gamma} \propto \frac{W_{\mathrm{gap}}}{r_{33}}\,\frac{v_{\mathrm{g,\,opt}}}{L} \propto \frac{W_{\mathrm{gap}}}{r_{33}}\,f_{3\,\mathrm{dB}}\,. \tag{7}$$

For the proportionality at the right-hand side of Eq. (7), the relations $\Gamma \propto 1/v_{\mathrm{g,\,opt}}$ and $f_{3\,\mathrm{dB}} \propto v_{\mathrm{g,\,opt}}/L$ were substituted from Eq. (6) and Eq. (3).

6. Optimized Mach-Zehnder modulator

For maximizing the modulation bandwidth $f_{3\,\mathrm{dB}}$, Eq. (3), of the MZM amplitude modulator and for minimizing its π-voltage U_π, Eq. (7), the optical group velocity $v_{\mathrm{g,\,opt}}$ of the PC line defect WG, its length L, the electro-optic coefficient r_{33} of the polymer, and the gap width W_{gap} need to be adjusted properly. For an integratable MZM with small length L, the design bandwidth $f_{3\,\mathrm{dB}}$ fixes the ratio $v_{\mathrm{g,\,opt}}/L$. Reducing $v_{\mathrm{g,\,opt}}$ then provides a small length L. It also needs to be considered that with lower $v_{\mathrm{g,\,opt}}$, the disorder-induced losses of the PC-WG increase [17] and the optical bandwidth decreases, so that $v_{\mathrm{g,\,opt}}$ cannot be made arbitrarily small.

For a small U_π, the electro-optic polymer is chosen to have a large linear electro-optic coefficient of $r_{33} = 80\,\mathrm{pm/V}$ [6]. Further, W_{gap} is chosen as small as compatible with the fabrication process. A gap width of $W_{\mathrm{gap}} = 150\,\mathrm{nm}$ can be fabricated to good accuracy with advanced litho-

Structure	r_2 / a	f_o (THz)	$v_{\mathrm{g,opt}}/c$	ɬ	L (σm)	$f_{3\mathrm{dB}}$ (GHz)
W1.4 dispersion large	0.3	196.4	2.4%	4.8	36	103
		196.6	3.4%	3.2	54	97
		196.9	4.8%	2.2	80	90
		196.2	6.4%	1.5	113	83
		197.7	8.2%	1.1	155	76
W1.25 dispersion flattened	0.38	197.5	3.2%	3.1	57	87
	0.36	**196.5**	**4.0%**	**2.2**	**80**	**78**
	0.34	195.8	5.2%	1.6	111	71
	0.32	195.2	6.6%	1.1	158	61
	0.30	194.6	7.9%	0.8	215	53

Table 1. Characteristic data for a PC slot waveguide modulator. Group velocity $v_{\mathrm{g,opt}}$, field interaction factor Γ, modulator length L and modulation bandwidth $f_{3\mathrm{dB}}$ are estimated at different optical carrier frequencies f_0. We assume an electro-optic coefficient of $r_{33} = 80\,\mathrm{pm/V}$. The modulation voltage amplitude for maximum extinction is fixed to $\hat{U} = U_\pi/4 = 1\,\mathrm{V}$.

#92415 - $15.00 USD Received 4 Feb 2008; revised 10 Mar 2008; accepted 10 Mar 2008; published 12 Mar 2008

graphic processes; hence this width is fixed for the present design. Given the gap width W_{gap}, the maximum modulation voltage amplitude is limited in practice by the microwave source and by dielectric breakdown in the gap.

In Table 1, we list group velocity $v_{\mathrm{g,\,opt}}$, field interaction factor Γ, modulator length L, and modulation bandwidth $f_{3\,\mathrm{dB}}$ for various PC slot waveguide modulators without (W1.4) and with dispersion flattening (W1.25), as already presented in Section 4. The π-voltage was kept fixed to $U_\pi = 4\,\mathrm{V}$ in all cases, which means that the modulation voltage amplitude $\hat{U} = U_\pi/4 = 1\,\mathrm{V}$ remained constant by adjusting the length L according to Eq. (7).

The values $v_{\mathrm{g,\,opt}}$ and Γ are calculated from simulations with the FIT method. As expected, the field interaction factor Γ increases and the modulator length L decreases when lowering the group velocity $v_{\mathrm{g,\,opt}}$ according to Eqs. (6), (7). The bandwidth $f_{3\,\mathrm{dB}}$ is calculated from Eq. (3) using the more exact numerical factor of 0.556 instead of 0.5. For a constant U_π the estimate Eq. (1) would predict a constant modulation bandwidth $f_{3\,\mathrm{dB}}$, however, it shows a weak $(1:1.4)$ dependence on $v_{\mathrm{g,\,opt}}$ $(1:3.4)$. This is explained after Eq. (6): The field interaction factor Γ is only approximately proportional to $1/v_{\mathrm{g,\,opt}}$, and therefore $U_\pi \propto v_{\mathrm{g,\,opt}}$ in Eqs. (7), (1) is an approximation, too. For the dispersion flattened structures, $f_{3\,\mathrm{dB}}$ is lower and shows a stronger dependence on $v_{\mathrm{g,\,opt}}$ compared to the structure with high dispersion.

The disorder-induced losses of a slow-light PC-WG operated at a group velocity of 5.8% of the vacuum speed of light were measured to be $4.2\,\mathrm{dB/mm}$ [18]. Doping silicon with a large concentration of phosphorus atoms ($2\times10^{18}\,\mathrm{cm}^{-3}$) leads to additional optical losses of only about $1\,\mathrm{dB/mm}$ [7]. At a slightly smaller group velocity of 4% of the vacuum speed of light and a moderate doping concentration of $2\times10^{16}\,\mathrm{cm}^{-3}$, optical losses will be mainly caused by disorder. With small device lengths the additional loss is expected to be tolerable.

Because the dispersion-flattened structure shows a large modulation bandwidth of $f_{3\,\mathrm{dB}} = 78\,\mathrm{GHz}$ at a length of only $L = 80\,\mu\mathrm{m}$ and for a small 1 V drive voltage amplitude, we regard this to be an optimum structure for the discussed technological constraints.

7. Slow-light coupling structure

Signals from an external fiber may be effectively coupled to a conventional strip WG mode with coupling losses below 1 dB [19]. However, an efficient method is also needed to excite the slow-light mode within the PC slot WG. We propose a coupling structure consisting of two sections, which are schematically shown in Fig. 5.

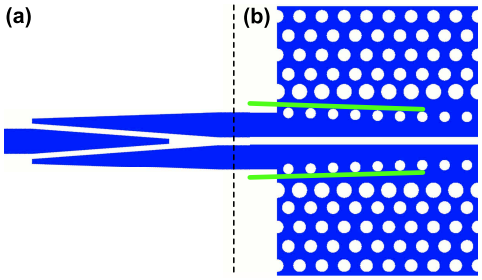

Fig. 5. Schematic of the coupling structure. (a) Transition from strip-WG to slot-WG (b) Coupling to PC WG. The transmission is significantly increased by introducing a PC taper, where the width W_1 of the PC-WG is slightly decreased from $1.45\sqrt{3}a$ to $1.25\sqrt{3}a$ over some lattice periods, indicated by the overlaid tilted (green) lines, and the width W_2 is increased from $0.55\sqrt{3}a$ to $0.65\sqrt{3}a$. The width of the strip-WG is 440 nm, and the gap width of both the slot-WG and the PC-WG is 150 nm.

#92415 - $15.00 USD Received 4 Feb 2008; revised 10 Mar 2008; accepted 10 Mar 2008; published 12 Mar 2008

The first section transforms[1] the strip WG mode into a slot-WG mode, Fig. 5(a). The design takes into account that the silicon on both sides of the gap needs to be electrically isolated as it is conductive and carries the modulation voltage, Fig. 2(a). FIT simulations of the strip-to-slot WG transition having a length of 7 μm predict a transmission loss lower than 0.3 dB and a reflection lower than -28 dB.

The second section couples the slot WG to the slow-light PC WG, Fig. 5(b). We developed a taper where the width of the PC WG is slightly decreased over a length of 10 periods (4.08 μm) to gradually slow down the PC WG mode. The calculated transmission and reflection curves are displayed in Fig. 6. The simulated structure comprises both the transition from a slot WG to a slow-light PC WG, Fig. 5(b), and the transition back to a slot WG.

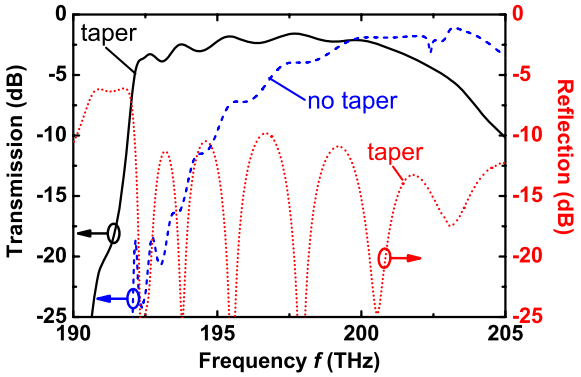

Fig. 6. Transmission and reflection for the transition from slot-WG to PC-WG and back to slot-WG, Fig. 5(b), with and without a PC taper. The introduction of the PC taper significantly enhances the transmission to a value better than -4 dB. The reflection is below -10 dB.

The transmission is better than -4 dB including both tapers, while it drops below -20 dB without tapers. The reflection stays below -10 dB. In the transmission curve with tapers, ripples can be observed. These are Fabry-Perot fringes generated by residual reflections at the interfaces. These reflections can be decreased by optimizing the transitions, and an extension of the taper sections lengths can further improve the device characteristics.

8. Conclusion

We propose a high-speed silicon modulator with low drive voltage based on a polymer-infiltrated slow-light photonic crystal line-defect waveguide. For a design with negligible first-order chromatic dispersion in an optical bandwidth of 1 THz we predict a modulation bandwidth of 78 GHz and a length of about 80 μm at a drive voltage amplitude of 1 V. This allows transmission at 100 Gbit/s.

[1] We thank an anonymous referee for pointing out a patent application, which describes such a structure: M. Lipson, C. A. Barrios, V. R. Almeida, R. R. Panepucci, and Q. Xu, United States Patent Application 20060228074.

#92415 - $15.00 USD Received 4 Feb 2008; revised 10 Mar 2008; accepted 10 Mar 2008; published 12 Mar 2008

Appendix

A. Field interaction factor Γ

For the derivation of the field interaction factor Γ we follow the formalism in [16]. The influence of the microwave field on the optical mode through the electro-optic effect is treated as a perturbation $\Delta\varepsilon$ on the permittivity of the material in Maxwell's equations

$$\nabla \times \mathbf{E} = -\mu \partial \mathbf{H}/\partial t\,, \tag{8}$$

$$\nabla \times \mathbf{H} = \partial[(\varepsilon + \Delta\varepsilon)\mathbf{E}]/\partial t\,. \tag{9}$$

For a mode propagating inside a PC WG along the z-direction, a complex envelope function A is defined,

$$\mathbf{E}(x,y,z,t) = A(z,t)\,\hat{\mathbf{E}}(x,y,z)\,\mathrm{e}^{\mathrm{j}(\omega_0 t - \beta_0 z)}, \tag{10}$$

$$\mathbf{H}(x,y,z,t) = A(z,t)\,\hat{\mathbf{H}}(x,y,z)\,\mathrm{e}^{\mathrm{j}(\omega_0 t - \beta_0 z)}\,. \tag{11}$$

The field distribution of the mode is taken at the optical carrier frequency $f_0 = \omega_0/(2\pi)$ and is assumed to be constant in the optical signal bandwidth centered at f_0. For the propagation constant β of the mode we assume $\beta(\omega) = \beta_0 + (\omega - \omega_0)v_{\mathrm{g,\,opt}}^{-1}$ neglecting chromatic dispersion. The orthogonality relation for two WG modes $\hat{\mathbf{H}}_{\mathrm{p,\,q}}$, $\hat{\mathbf{E}}_{\mathrm{p,\,q}}$ subscripted with p and q, respectively, and having the same frequency can be derived following [20],

$$\int (\hat{\mathbf{E}}_{\mathrm{q}} \times \hat{\mathbf{H}}^*_{\mathrm{p}} - \hat{\mathbf{H}}_{\mathrm{q}} \times \hat{\mathbf{E}}^*_{\mathrm{p}}) \cdot \mathbf{e}_z \,\mathrm{d}A = 4\delta_{\mathrm{pq}} P_{\mathrm{p}}\,. \tag{12}$$

Here, δ_{pq} is the Kronecker delta, P_{p} is the cross-section power of mode p, and the integration is performed over a cross-section perpendicular to the propagation direction. If Eqs. (10), (11) are substituted in Eqs. (8), (9), and both the mode orthogonality condition Eq. (12) and the slowly varying envelope approximation are used, a nonlinear propagation equation is obtained,

$$\frac{\partial A}{\partial z} + \frac{1}{v_{\mathrm{g,\,opt}}}\frac{\partial A}{\partial t} = \mathrm{j}\,\omega_0 \Gamma K U A, \qquad A = |A|\,\mathrm{e}^{\mathrm{j}(\Phi + \Delta\Phi)}\,. \tag{13}$$

In Eq. (13), the relations $A = A(z,t)$, $U = U(z,t)$, $\Phi = \Phi(z,t)$ and $\Delta\Phi = \Delta\Phi(z,t)$ hold. The field interaction factor Γ is defined in Eq. (6), $K = \frac{\varepsilon_0}{2} r_{33} n_{\mathrm{poly}}^3 Z_0 / W_{\mathrm{gap}}$ is a constant, and $U = U(z,t)$ is the voltage across the gap. It is generated by the microwave field that causes an electro-optic refractive index change $\Delta n = -r_{33} n_{\mathrm{poly}}^3 U / W_{\mathrm{gap}}$ and a resulting phase change $\Delta\Phi$.

B. Relation between field interaction factor Γ *and group velocity* $v_{\mathrm{g,opt}}$

We first sketch the derivation of the dependence of the power flow on group velocity. Observing that the nonlinear perturbation of the permittivity is small, $\Delta\varepsilon \ll \varepsilon$, we substitute the modal fields Eqs. (10), (11) with $A = 1$ into Eq. (11) and obtain

$$\nabla \times \hat{\mathbf{H}} - \mathrm{j}\,\beta_0 \mathbf{e}_z \times \hat{\mathbf{H}} = \mathrm{j}\,\omega_0 \varepsilon \hat{\mathbf{E}}\,. \tag{14}$$

From this equation, we write the total differential with respect to the variables β_0 and ω_0 and find

$$-\,\mathrm{d}\,\beta_0 (\mathbf{e}_z \times \hat{\mathbf{H}}) = \mathrm{d}\omega_0 \varepsilon \hat{\mathbf{E}}\,. \tag{15}$$

We form the scalar product of the complex conjugate of Eq. (15) with $\hat{\mathbf{E}}$ and the scalar product of Eq. (15) with $\hat{\mathbf{E}}^*$. Then we add both relations, observe $(\mathbf{e}_z \times \hat{\mathbf{H}}^*) \cdot \hat{\mathbf{E}} = (\hat{\mathbf{H}}^* \times \hat{\mathbf{E}}) \cdot \mathbf{e}_z = -(\hat{\mathbf{E}} \times \hat{\mathbf{H}}^*) \cdot \mathbf{e}_z$, and integrate over a volume $V = aA$ with differential $dV = a\,\mathrm{d}A$, where $\mathrm{d}A$ is the

#92415 - $15.00 USD Received 4 Feb 2008; revised 10 Mar 2008; accepted 10 Mar 2008; published 12 Mar 2008

differential of the cross-section area A in a plane $z = \text{const}$. For PC WGs, the length a along the waveguide's z-axis corresponds to the size of the unit cell. We find

$$\mathrm{d}\beta_0 \int \tfrac{1}{4}(\hat{\mathbf{E}} \times \hat{\mathbf{H}}^* + \hat{\mathbf{E}}^* \times \hat{\mathbf{H}}) \cdot \mathbf{e}_z \, \mathrm{d}V = \mathrm{d}\omega_0 \int \tfrac{1}{2}\varepsilon |\hat{\mathbf{E}}|^2 \, \mathrm{d}V \,. \tag{16}$$

The right-hand side integral of Eq. (16) is the mean stored energy at frequency f_0 inside the volume under consideration. The integrand on the left-hand side of Eq. (16) is the real part of the z-component of the complex Poynting vector $\frac{1}{2}\hat{\mathbf{E}} \times \hat{\mathbf{H}}^*$. Its integral over the cross section area A is independent of the z-position. So the volume integral may be written as an integral over the cross-section multiplied by the length a of the volume along z. The result is

$$\frac{1}{v_{\mathrm{g,\,opt}}} = \frac{\mathrm{d}\beta_0}{\mathrm{d}\omega_0} = \frac{\int \frac{1}{2}\varepsilon |\hat{\mathbf{E}}|^2 \, \mathrm{d}V}{a \int \Re(\frac{1}{2}\hat{\mathbf{E}} \times \hat{\mathbf{H}}^*) \cdot \mathbf{e}_z \, \mathrm{d}A} \,. \tag{17}$$

Equation (17) can be understood intuitively: The energy stored in a volume $V = aA$ per transit time $a/v_{\mathrm{g,\,opt}}$ of the wave that crosses this volume equals the cross-section power. Thus for a fixed amount of transmitted power, the stored energy increases inversely proportional to the group velocity. Relation (17) resembles but is distinct from the field confinement factor Eq. (6), where the power in the waveguide core is related to the total cross-section power: The more power is concentrated to the core, the larger the propagation constant becomes, and the slower the wave propagates.

C. Modulator bandwidth limitations by RC-effects

We estimate the modulator bandwidth limitations that are caused by electrical *RC*-effects. We discuss two different mechanisms that reduce the electrical voltage drop across the gap and lead to an associated 3 dB bandwidth. These are the generator-determined bandwidth and the parallel-loss determined bandwidth. We find that these bandwidth limitations do not play a significant role for the presented structures.

For the following numerical examples, the data of our specific MZM design for a 78 GHz modulation bandwidth and a drive voltage of 1 V were assumed, Fig. 1 and Fig. 2: Optical strip waveguide height $h = 220\,\mathrm{nm}$, PM section length and gap width $L = 80\,\mu\mathrm{m}$ and $W_{\mathrm{gap}} = 150\,\mathrm{nm}$, linear refractive index of the PM section $n_{\mathrm{poly}} = 1.6$ (assumed to be the same at optical and electrical frequencies), width of the doped silicon slabs $w = 3\,\mu\mathrm{m}$, vacuum dielectric constant ε_0, vacuum speed of light c.

1) Generator-determined bandwidth

The CPWG with wave impedance $Z_{\mathrm{L}} = 50\,\Omega$ be terminated with an open, Fig. 7(a). We assume the PM section to be short compared to the modulation signal wavelength, so that the CPWG may be represented by a lumped gap capacitance $C_{\mathrm{gap}} = \varepsilon_0 n_{\mathrm{poly}}^2 hL/W_{\mathrm{gap}}$ for each PM. The voltage amplitude U_{gap} across the non-conductive gap W_{gap} (i. e., across the lumped capacitor $2C_{\mathrm{gap}}$) decreases with modulation frequency f because of the generator impedance $R_{\mathrm{G}} = 50\,\Omega$,

$$\frac{U_{\mathrm{gap}}}{U_{\mathrm{G}}} = \frac{1}{1 + \mathrm{j}\,\omega R_{\mathrm{G}} 2C_{\mathrm{gap}}}, \qquad f_{3\,\mathrm{dB}}^{(R_{\mathrm{G}}C_{\mathrm{gap}})} = \frac{1}{4\pi R_{\mathrm{G}} C_{\mathrm{gap}}} \,. \tag{18}$$

At the limiting frequency $f_{3\,\mathrm{dB}}^{(R_{\mathrm{G}}C_{\mathrm{gap}})}$ the gap voltage $|U_{\mathrm{gap}}|$ drops to $|U_{\mathrm{G}}|/\sqrt{2}$. Assuming the previously assigned data and neglecting electric fringing fields, the total gap capacitance amounts to $2C_{\mathrm{gap}} = 5\,\mathrm{fF}$, and $f_{3\,\mathrm{dB}}^{(R_{\mathrm{G}}C_{\mathrm{gap}})} \approx 640\,\mathrm{GHz}$ results. In view of the envisaged MZM bandwidth of 78 GHz, the generator-determined limitation is unimportant.

#92415 - $15.00 USD Received 4 Feb 2008; revised 10 Mar 2008; accepted 10 Mar 2008; published 12 Mar 2008

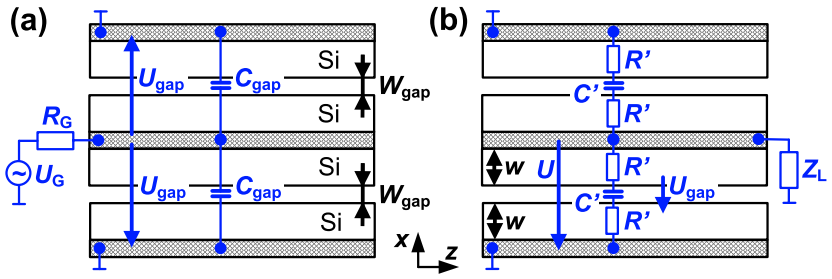

Fig. 7. Electrical *RC*-effects. (a) Generator-determined limitation (b) Parallel-loss determined limitation. In (a), the electrically short PM section is represented by a lumped gap capacitance C_{gap}, and the voltage across the gap U_{gap} is only a fraction of the generator voltage U_{G} because of the generator impedance R_{G}. In (b), a voltage wave with constant amplitude $|U|$ travels in z-direction. The voltage U_{gap} across the gap (capacitance per length C') is reduced because of the finite resistivity of the doped silicon sections of width w (conductance per length (R'^{-1}).

2) Parallel-loss determined bandwidth

The CPWG be terminated with its wave impedance Z_{L}, Fig. 7(b). Then, a modulating electrical wave traveling in z-direction has a spatially constant amplitude $|U|$. The resulting voltage amplitude $|U_{\mathrm{gap}}|$ across the non-conductive gap W_{gap} (PM capacitance per length $C' = \varepsilon_0 n_{\mathrm{poly}}^2 h/W_{\mathrm{gap}}$) is reduced because of the finite resistivity of the doped silicon. For silicon sections having a width w and a filling factor F taking the reduction of the effective conductance by the air holes into account (conductance per length $(R'^{-1} = \sigma F h/w)$, we obtain

$$\frac{U_{\mathrm{gap}}}{U} = \frac{1}{1+\mathrm{j}\,\omega 2R'C'}, \qquad f_{3\,\mathrm{dB}}^{(R'C')} = \frac{1}{4\pi R'C'} \tag{19}$$

The limiting frequency $f_{3\,\mathrm{dB}}^{(R'C')}$ denotes where the gap voltage $|U_{\mathrm{gap}}|$ drops to $|U|/\sqrt{2}$. Assuming a conductivity $\sigma = 10\,\Omega^{-1}\,\mathrm{cm}^{-1}$ of the doped ($n_{\mathrm{D}} \approx 2\times 10^{16}\,\mathrm{cm}^{-3}$) silicon material and a filling factor $F = 0.67$, a bandwidth of $f_{3\,\mathrm{dB}}^{(R'C')} \approx 120\,\mathrm{GHz}$ results. In view of the envisaged MZM bandwidth of 78 GHz, the parallel-loss determined limitation does not play a significant role either.

3) Other effects

Basically, one might think of a bandwidth limitation by the finite carrier transit time in the doped silicon slabs, see Fig. 2. This carrier drift time is determined by the slower carriers, which in silicon are holes, the maximum saturation velocity of which is about $0.6\times 10^7\,\mathrm{cm/s}$. Over the $3\,\mu\mathrm{m}$ witdh of the silicon slab, this would lead to a response time in the order of $\tau_{\mathrm{D}} = 50\,\mathrm{ps}$, resulting in a bandwidth in the order of 3 GHz only.

However, there is also the dielectric dielectric relaxation time τ_{R}, inside which any charge perturbation in the doped silicon slabs (induced by the modulating field) is screened by a shift of the whole carrier ensemble. The dielectric relaxation time $\tau_{\mathrm{R}} = \varepsilon_0\,\varepsilon_{\mathrm{r}}/\sigma$ depends on the material's conductivity σ and permittivity $\varepsilon_0\,\varepsilon_{\mathrm{r}}$. For $\sigma = 10\,\Omega^{-1}\,\mathrm{cm}^{-1}$ as assumed above and with $\varepsilon_{\mathrm{r}} = 12$, a value of $\tau_{\mathrm{R}} = 0.1\,\mathrm{ps}$ is obtained.

For the resulting response time $\tau_{\mathrm{res}}^{-1} = \tau_{\mathrm{D}}^{-1} + \tau_{\mathrm{R}}^{-1} \approx \tau_{\mathrm{R}}^{-1}$, the *faster* of the two effects is relevant, and the bandwidth limited by the dielectric relaxation time would be 1.6 THz. As a consequence, carrier transit times do not limit the modulator's performance.

#92415 - $15.00 USD Received 4 Feb 2008; revised 10 Mar 2008; accepted 10 Mar 2008; published 12 Mar 2008

Acknowledgment

This work has been supported by the Deutsche Telekom Stiftung, by the Deutsche Forschungsgemeinschaft (DFG) in the framework of the Priority Program SP 1113 “Photonic Crystals“ and by the Center of Functional Nanostructures (CFN) within projects A3.1 and A4.4.

#92415 - $15.00 USD Received 4 Feb 2008; revised 10 Mar 2008; accepted 10 Mar 2008; published 12 Mar 2008